INEEL/EXT-01-00913
Revision 1

Multi-Megawatt Power System Trade Study

G. R. Longhurst
B. G. Schnitzler
B. T. Parks

November 2001

Idaho National Engineering and Environmental Laboratory
Bechtel BWXT Idaho, LLC

INEEL/EXT-01-00913
Revision 1

Multi-Megawatt Power System Trade Study

Glen R. Longhurst
Bruce G. Schnitzler
Benjamin T. Parks

November 2001

Idaho National Engineering and Environmental Laboratory
Idaho Falls, Idaho 83415

Prepared for the
U.S. Department of Energy
Assistant Secretary for Nuclear Energy
Under DOE Idaho Operations Office
Contract DE-AC07-99ID13727

ABSTRACT

As part of a larger task, the Idaho National Engineering and Environmental Laboratory (INEEL) was tasked to perform a trade study comparing liquid-metal cooled reactors having Rankine power conversion systems with gas-cooled reactors having Brayton power conversion systems. This report summarizes the approach, the methodology, and the results of that trade study. Findings suggest that either approach has the possibility to approach the target specific mass of 3-5 kg/kW_e for the power system, though it appears either will require improvements to achieve that. Higher reactor temperatures have the most potential for reducing the specific mass of gas-cooled reactors but do not necessarily have a similar effect for liquid-cooled Rankine systems. Fuels development will be the key to higher reactor operating temperatures. Higher temperature turbines will be important for Brayton systems. Both replacing lithium coolant in the primary circuit with gallium and replacing potassium with sodium in the power loop for liquid systems increase system specific mass. Changing the feed pump turbine to an electric motor in Rankine systems has little effect. Key technologies in reducing specific mass are high reactor and radiator operating temperatures, low radiator areal density, and low turbine/generator system masses. Turbine/generator mass tends to dominate overall power system mass for Rankine systems. Radiator mass was dominant for Brayton systems.

CONTENTS

FIGURES

TABLES

MULTI-MEGAWATT POWER SYSTEM TRADE STUDY

CHARTER

As part of the Special Purpose Fission Technology (SPFT) program conducted by the U. S. Department of Energy's Office of Nuclear Energy, Science and Technology, (DOE-NE), the INEEL was chartered to

- Review past multi-megawatt (MMW) concepts and studies,[1]
- Compare current requirements for a MMW system, working in coordination with the National Aeronautics and Space Administration (NASA),
- Update one or two previous concepts and or define a new concept for a MMW system that is compatible with the Variable Specific Impulse Magnetoplasma Rocket (VASIMR) engine concept,[2]
- Assess long-lead technologies that would need to be worked on to support development of such a system,
- State performance levels (efficiencies, operating temperatures, etc.) that would be required of these technologies, and
- Identify technical issues associated with development that would need to be addressed as part of a technology development program.

Supplemental guidance[3] was:

"The MMW Concept Team is to develop a concept trade study table …. Both gas-Brayton and liquid-metal-Rankine options being considered should be listed. Following development of the table, the MMW concept team is requested to perform a trade study of the two concepts. This trade study should provide the following information:

– *Concept information* requested in Figure 5, Section 3, of the Design Data Request (DDR)[4] issued by Oak Ridge National Laboratory (ORNL)
– *Initial numerical estimates* for mass, deployed volume and specific mass in a form consistent with DDR Table 5.23
– *Qualitative information* addressing Evaluation Criteria (EC) numbers 9, 10, 11, and 16 of the DDR. Detailed answers to the questions associated with each criterion are not expected. However, a short narrative summary addressing the topical areas, providing qualitative information and any readily available quantitative information is desired.

This report documents work on the task to perform an initial concept trade study.

CONCEPT TRADE STUDY SET

Two main classes of power systems were considered. One uses a liquid-metal-cooled reactor and a liquid/vapor metal Rankine cycle power conversion system. That system is shown schematically in Figure 1. The other uses Brayton cycle power conversion, but includes both gas-cooled and liquid-metal-cooled reactors. The gas-cooled configuration is shown schematically in Figure 2. Working within the guidelines provided, the INEEL MMW team prepared the initial concept set table, listed here as Table 1.

In each case, two levels of availability were assumed regarding reactor fuel technology. The first was relatively state-of-the art technology (which still may require considerable work to achieve), while the second was a "growth" or advanced technology.

For liquid metal cooled reactors, the near-term technology was UN fuel in Nb-1Zr cladding with a reactor coolant exit temperature of 1,350 K, as called for in the SP-100 design.[5] The "growth" option assumed a cladding change to ASTAR 811C, which is

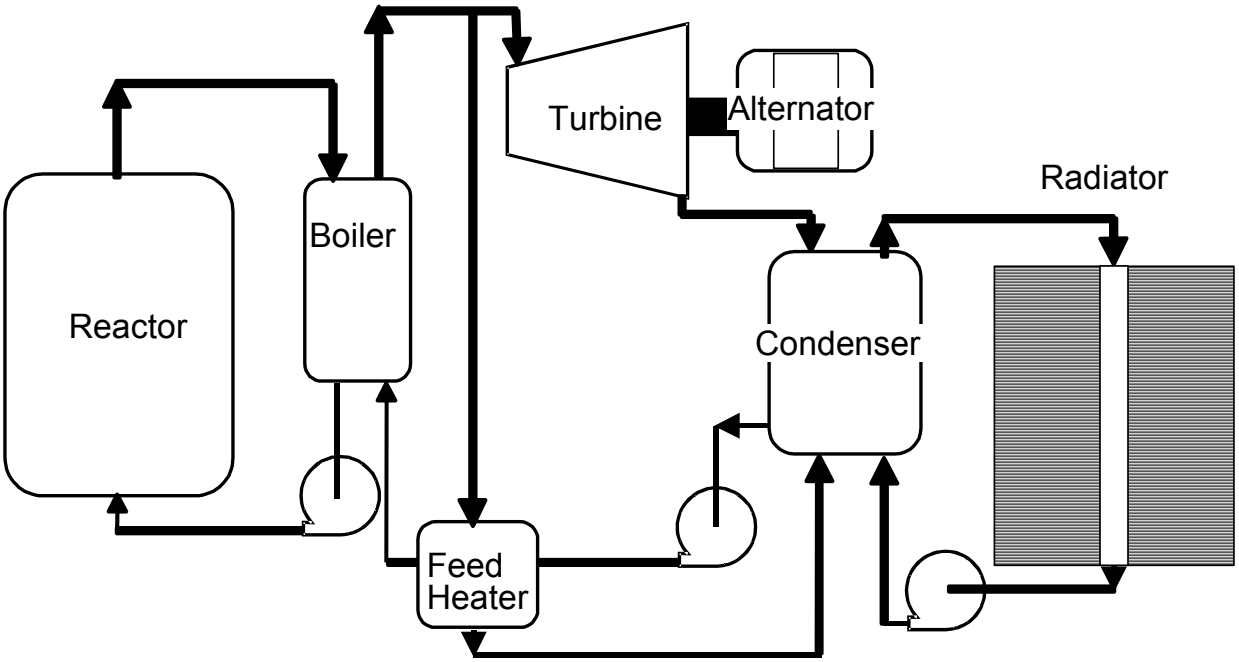

Figure 1. Schematic of Rankine power system analyzed using the ALKASYS code.

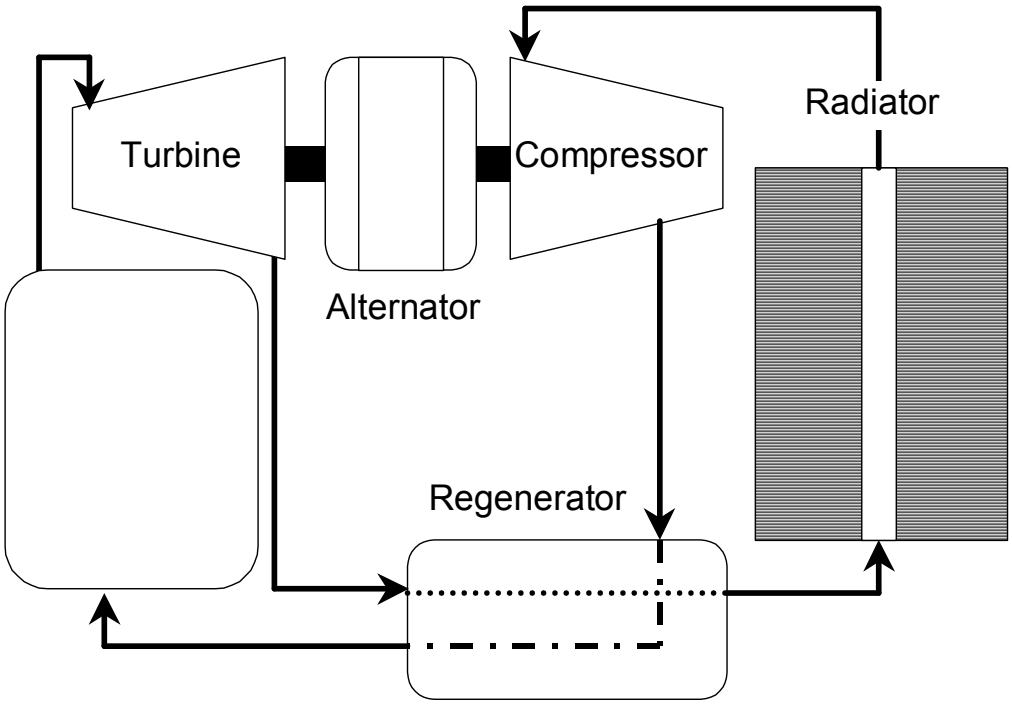

Figure 2. Schematic showing basic elements of a Brayton cycle power system.

Table 1. Concept Trade Study Set developed for Multi-Megawatt Power System.

Concept	Fuel	Clad/ Coating	Neutron Spectrum	Reactor Cooling	Fluid Temp (K)	Power Conversion	Heat Rejection Mechanism	Power Level	Technology Base
Rankine:									
UN/Nb-1Zr/Li-K	UN	Nb-1Zr	Fast	Li	1,350	K-Rankine	Heat Pipe Radiator	15 MWe	SP-100
UN/Nb-1Zr/Ga-K	UN	Nb-1Zr	Fast	Ga	1,350	K-Rankine	Heat Pipe Radiator	15 MWe	SP-100
UN/Nb-1Zr/Li-Na	UN	Nb-1Zr	Fast	Li	1,350	Na-Rankine	Heat Pipe Radiator	15 MWe	SP-100
UN/Nb-1Zr/Ga-Na	UN	Nb-1Zr	Fast	Ga	1,350	Na-Rankine	Heat Pipe Radiator	15 MWe	SP-100
UN/ASTAR 811C/Li-K	UN	ASTAR 811C	Fast	Li	1,500	K-Rankine	Heat Pipe Radiator	15 MWe	SP-100 Growth
UN/ASTAR 811C/Ga-K	UN	ASTAR 811C	Fast	Ga	1,500	K-Rankine	Heat Pipe Radiator	15 MWe	SP-100 Growth
UN/ASTAR 811C/Li-Na	UN	ASTAR 811C	Fast	Li	1,500	Na-Rankine	Heat Pipe Radiator	15 MWe	SP-100 Growth
UN/ASTAR 811C/Ga-Na	UN	ASTAR 811C	Fast	Ga	1,500	Na-Rankine	Heat Pipe Radiator	15 MWe	SP-100 Growth
Brayton:									
UC_2/NbC	UC_2	NbC	Thermal	He-Xe	1,640	He-Xe Brayton	Heat Pipe Radiator	15 MWe	NERVA Derivative
UC_2/NbC IHX	UC_2	NbC	Thermal	He-Xe	1,640	Brayton Indirect	Heat Pipe Radiator	15 MWe	Intermediate Heat Exchanger
UC_2/ZrC	UC_2	ZrC	Thermal	He-Xe	1,920	He-Xe Brayton	Heat Pipe Radiator	15 MWe	NERVA Derivative Growth
UO_2/SiC	UO_2	SiC	Thermal	He-Xe	1,520	He-Xe Brayton	Heat Pipe Radiator	15 MWe	Commercial HTGR
UO_2/ZrC	UO_2	ZrC	Thermal	He-Xe	2,100	He-Xe Brayton	Heat Pipe Radiator	15 MWe	Advanced HTGR
UN/Nb-1Zr/Li	UN	Nb-1Zr	Fast	Li	1,350	He-Xe Brayton	Heat Pipe Radiator	15 MWe	SP-100

believed to allow a reactor coolant exit temperature of 1,500 K.

For the gas-cooled reactors, we chose as a reference the NERVA Derivative technology.[6] As a baseline, we chose UC_2 (coated uranium carbide particles in a graphite matrix) fuel with NbC coating, with an assumed gas exit temperature of 1,640 K. "Growth" options examined included UC_2 fuel with ZrC coating and UO_2 with SiC and ZrC coatings. Reactor outlet temperatures assumed ranged from 1,520 K for the UO_2/SiC option to 2,100 K for the UO_2/ZrC option.

A final case considered a liquid-cooled reactor operating a Brayton system through a heat exchanger. It used UN fuel with Nb-1Zr cladding. Reactor outlet temperature for this system was 1,350 K.

APPROACH

We evaluated these concepts in terms of their specific masses, counting all the elements of the power system, including the reactor, shield, power conversion, power management and distribution (PMAD), and heat rejection systems. The masses did not include that of the VASIMR engine, which will be included when progress toward the overall goal of 3–5 kg/kW_e is evaluated.

Liquid cooled reactor masses and masses of Rankine power conversion systems were estimated using ALKASYSM, a modified version of the ALKASYS-PC code[7] written at Oak Ridge National Laboratory in the late 1980s for analysis of liquid-metal Rankine cycle space power systems. Built into it are scaling laws for the various components of such systems given power required, operating temperatures, and material properties. We modified the ALKASYS-PC code by adding flexibility to make use of other fluids than lithium and potassium as either primary coolant or working fluid, and to use an optional electric motor to operate the boiler feed pump in lieu of the vapor-driven turbine assumed in the code. The temperature at which structural material changed from Nb-1Zr to ASTAR 811C was also made arbitrary, and an option was added to allow blade tip velocity to be specified as a Mach number. As written, ALKASYS-PC assumes potassium as the working fluid in the power system and that either (1) the potassium is boiled directly in the reactor, or (2) molten lithium in the reactor boils the potassium in a boiler. Reactor materials assumed are Nb-1Zr structure for reactor temperatures less than a specified value, originally 1100 K, and the tantalum alloy ASTAR 811C above that. Fuel cladding is assumed in the code to be ASTAR 811C at all temperatures. The difference in overall reactor mass in accepting this assumption as compared with using Nb-1Zr density for the low-temperature cladding is inconsequential. For details regarding that code conversion see Ref. [8].

Gas-cooled reactor masses were based on the Enabler NERVA Derivative reactor design[6] using a polynomial fit to interpolate mass estimates at 5, 10, 40, and 70 MW_e to the 15 MW_e power used as a basis for comparison here. Scaling to different operating temperatures than 1,920 K given as the Enabler gas exit temperature was based on the assumptions that

1. Reactor overall mass density and configuration would remain essentially constant,
2. Reactor volume would increase as the 3/2 power of flow areas required to carry thermal power,
3. Thermal power from the reactor would change with thermodynamic efficiency of the Brayton systems connected to them,
4. Flow velocities and gas pressures would remain constant.

Thus, our simple scaling law for temperature variations is

$$M_r \propto \left(\frac{T_e}{\eta_{th}} \right)^{\frac{3}{2}} \qquad (1)$$

where

M_r = Reactor mass
T_e = Coolant exit temperature
η_{th} = Power conversion system thermal efficiency.

Brayton power conversion system analyses were performed by Dr. Lee Mason, NASA Glenn Research Center (GRC).[9] His results included

cycle thermodynamic efficiency for each of the Brayton systems identified in Table 1. They also included, among other things, compressor pressure ratio, turbine temperature ratio, radiator area, heat exchanger mass (when used), power conversion system mass, heat rejection system mass, and power management and distribution system (PMAD) system mass.

Shield masses depend not only on reactor size and source strength, but also on the protection required, the area to be protected, and its position relative to the source. Our basis for this comparison was that used in the SP-100 study: an area located 22.5 m from the center of the reactor required gamma doses not to exceed 5×10^5 rad and the fast neutron (1 MeV equivalent) fluence not to exceed 1×10^{13} n/cm^2 over a 7 year operating life. These are representative values for protection of near-term electronics and not for biological protection.

For liquid metal cooled reactors, shield masses were estimated using ALKASYSM logic, which is based on Refs. (10–12) We chose the SP-100 circular shielded area 4.5 m in diameter . For gas-cooled reactors, shield masses were scaled from the Enabler NERVA Derivative design. There, shield masses were based on a gamma dose of only 5 rad/yr at a distance of 100 m from the reactor. Polynomial-interpolation of published data for powers around 15 MW_e was used to scale to 15 MW_e under those same constraints. The resulting shield mass $M_{s_{Enabler}}$ was 11,100 kg. We used $1/r^2$ scaling on dose to relocate the protected area from 100 m to the 22.5-m position and the logic for shield thickness determination in ALKASYSM to scale from the shifted Enabler design dose to the reference doses. We then scaled for reactor size variations with reactor volume to the 2/3 power. Thus, our simplified scaling law for gas-cooled reactor shield mass is

$$M_s = M_{s_{Enabler}} \times 0.4 \times \left(\frac{T_e}{1920}\right)\left(\frac{0.276}{\eta_{th}}\right) \qquad (2)$$

Thermal radiators in both system classes were assumed to have an areal mass density of 6 kg/m^2 (planform). Assuming two-sided radiators, the effective value was 3 kg/m^2 (radiating). That is an improvement over the nominally 20 kg/m^2 found in ALKASYSM results, but it is substantiated by our independent heat pipe radiator parametric study summarized in Appendix A. For reference, the areal density of the complete radiator system in the SP-100 design was about 3–4 kg/m^2 of one-sided radiating area for the heat pipes and 11.7 kg/m^2 for the pumped lithium heat transport system to couple the heat pipe radiator to the power conversion working fluid.[13] Further discussion of that choice of value is in Appendix A. Areas required to radiate the waste heat as calculated in the respective models were accepted. That included a primary radiator to reject power conversion process heat and a second, lower temperature radiator for cooling the shield and power conversion electronics.

Masses for the power management and distribution (PMAD) system, sometimes referred to as the power conversion system, were assumed to be the same for both systems. The 15,106-kg value in the GRC analyses was considered more realistic and was used for both systems. PMAD and parasitic load heat rejection mass was included in the PMAD system mass for both system types.

We assumed as a baseline that both system types used four turbine/generator sets, though examination of a two-turbine set was performed for the Rankine system.

For other components, masses found by the GRC Brayton analysis were assumed for Brayton systems, and those generated by ALKASYSM were accepted for the Rankine systems.

MODELING ASSUMPTIONS

Here we discuss the pertinent specific assumptions made in the modeling analyses performed beyond those mentioned above.

Brayton Systems

The following assumptions were made in performing the GRC analyses on the Brayton system cases in Table 1.

- For the liquid-metal-cooled option in the Brayton system analysis, SP-100 technology

was assumed with its reactor coolant exit temperature of 1350 K.

- The heat exchangers for gas-to-gas and metal-to-gas heating of the working gas were assumed 95 percent efficient.
- Mass optimized temperature ratio (turbine inlet/compressor inlet) and compressor pressure ratio were assumed.
- Power conversion masses included turbines, alternators, compressors, recuperators, waste heat exchanger, ducts, and a 10 percent engine structure mass fraction.
- The working fluid was assumed a mixture of He and Xe with a molecular weight of 40.
- Efficiencies assumed were

  Turbines 90 percent

  Compressors 80 percent

  Recuperators 95 percent

  Pressure ratio loss fraction 5 percent (95 percent efficiency).
- The liquid-to-gas heat exchanger was assumed to have a 1.2 heat capacity ratio.
- Power conversion waste heat was assumed to be rejected through the main radiators. The radiation shield was assumed cooled by the secondary radiator.
- Alternators were assumed to have

  95 percent efficiency

  1 kHz, 3 phase, 1000 V_{rms} output

  Liquid-cooled stator with waste heat rejected by the Brayton system secondary radiator.
- PMAD mass was assumed to include

  Filter

  Connectors

  Enclosures

  Engine controller

  Parasitic load radiator (resistance used to stabilize electric load on alternator)

  Waste heat radiator with Parasitic load radiator temperature of 500°C

  50 m of cabling
- The filter was assumed to have

  Filter efficiency of 99 percent

  Cold plate temperature of 60°C

  Transmission efficiency of 98 percent.

Rankine Systems

Parameters other than fluid properties that were included in the ALKASYSM input data file include the following. Units for these data are mixed SI and English, as called for by the code.

Reactor Type

The base case assumed a separately cooled reactor with lithium as the primary coolant. Variations included direct boiling potassium and sodium as well.

Boiler Outlet Temperature

We arbitrarily assumed that vapor quality leaving the boiler was 1.0, but the outlet temperature was an open parameter varied in the course of analysis. It is limited by the maximum temperature allowed in the fuel and cladding in the reactor. For the direct boiling configuration, this was taken as the reactor-coolant outlet temperature. In the case of separate primary coolant and working fluid, the boiler outlet temperature was reduced to keep reactor outlet temperature at its predetermined value.

Condenser

The condensing temperature of the coolant in the condenser was an arbitrarily specified parameter. It strongly influences the system specific mass through the radiator area required to reject the required heat. Values we used in the comparison ranged from 600–1000 K. We chose 800 K as the baseline case. Also specified for the condenser is the amount of sub-cooling at the condenser outlet. While the condensing temperature determines through the fluid properties the pressure in the condenser, and therefore at the turbine outlet, the sub-cooling determines the out-

let temperature for the condenser. We assumed 6 K (10°R) of sub-cooling.

Radiators

Heat loads from electronics and from some other lower temperature sources are assumed in ALKASYSM to be rejected through a low-temperature radiator. Because the radiators are the largest components in physical dimensions, a key issue is whether they will fit in the cargo bay of a launch vehicle. ALKASYSM makes a determination on whether or not a radiator will fit into the specified cargo bay using specific configuration assumptions based on total area required. For the MMW systems considered here, that form was a three finned design. Required parameters associated with the radiators, together with the values used for the present comparison are arbitrarily chosen as follows:

Low-temperature radiator temperature (K)	600
Launch bay diameter (ft)	23
Launch bay length (ft)	72.2

Even though ALKASYSM generates an estimate of radiator mass based on empirical correlations, for purposes of comparison, we chose the constant radiator areal density of 6 kg/m^2 (planform) suggested by SP-100 and the analysis in Appendix A.

Boiler Feed Heaters

Most computations were performed assuming just one stage of feed heating, but other values were also examined.

Another required parameter is the feed heater terminal temperature difference. Counter-flow heat exchangers are assumed, and this difference is that between the inlet temperature of the heating fluid and the outlet temperature of the heated fluid. The value of 6 K (10°R) was used here. At the other end of the heater, the specified drain cooler terminal temperature difference is that between the heating fluid outlet temperature and the heated fluid inlet temperature. The value of 12 K (20°R) was assumed for that.

Main Turbine/Generator

Besides the number of turbine/generator units, required inputs for the turbine with the values assumed include

Turbine dry stage efficiency	0.90
Turbine exhaust loss (BTU/lbm)	5
Turbine last stage tip Mach number	< 0.6

Generator inputs required include

Net system electrical output (kW_e)	15,000
Generator efficiency	0.95

The turbine and generator masses computed by ALKASYSM depend on turbine rotational speed, which, in turn, is controlled by the specified last stage tip velocity as discussed below in Appendix B. A code option in ALKASYSM is to supply blade tip Mach number in lieu of a set velocity. Assuming that the blade pitch diameter is 1.5 times the hub diameter, it makes sense to limit the tip velocity to a Mach number less than 0.6, thus ensuring subsonic flow from the nozzles under the assumption that the spouting velocity is 1.5 times the tip velocity. The amount less is determined by the Hudson blade root stress (see Appendix B). We assumed it could not exceed 40,000 psi (276 MPa).

Feed Pump

ALKASYS-PC regards the feed pump and its driving turbine as an integrated unit, but as indicated previously, our adaptations have allowed replacement of the pump turbine with an electric motor of equivalent mass. Besides specifying pump type, specific parameters input with their values are

Pump drive turbine efficiency	0.9
Feed pump efficiency	0.6
Temperature drop through pump drive turbine (°R)	350

When the electric-motor option is selected, the first of these is assumed to be the motor efficiency while the last parameter, temperature

drop, is inconsequential. We performed most calculations with drive turbines assumed, but some were done with the electric motors assumed.

Reactor/Boiler

Parameters related to the reactor, and if used to the boiler, with the values assumed are

Boiler feed subcooling (°R)	200
Fraction of electrical output to drive primary coolant pump	0.01
System full power life (yr)	7
Flow velocity in vapor lines (ft/s)	450
Flow velocity in wet mixture lines (ft/s)	100
Flow velocity in liquid lines (ft/s)	10
Heater tube outside diameter (in)	0.25
Heater tube wall thickness (in)	0.020

Other

The remaining parameters required are the jet-pump flow ratio (flow through the Venturi nozzle to that drawn in by the Bernoulli effect from the reservoir being drained) for the jet pumps used, and the temperature at which structural material is assumed to change from Nb-1Zr to ASTAR 811C. The value of 4.0 was used for the jet pump flow ratio, and 1,360 K was taken as the material transition temperature.

RESULTS

In this section we present the results of calculations performed to evaluate the overall specific mass (kg/kW_e) for the two general configurations investigated. Table 2 compares results for two baseline cases selected: (1) direct heated gas using NERVA Derivative reactor technology for the Brayton system, and (2) lithium-cooled SP-100 reactor technology with potassium as the working gas in a Rankine system and a condenser temperature of 800 K.

Table 2. Parameter comparison for the two baseline comparison cases.

Parameter	Gas Brayton Baseline	Liquid Rankine Baseline
Turbine inlet temperature (K)	1,640	1,260
Reactor thermal power (kW_t)	61,579	59,108
Thermal efficiency (%)	24.4	25.4
Reactor mass (kg)	6,648	14,654
Shield mass (kg)	4,290	9,709
Heat exchanger mass (kg)	0	2,254
Turbine/generator mass (kg)	4,480	43,614
Main radiator temperature (K)	746-541	756
Main radiator area (m^2)	5,563	3,379
Secondary radiator area (m^2)	1,899	283
Total radiator mass (kg)	22,386	11,039
Power conditioning mass (kg)	15,106	15,106
Total mass (kg)	52,910	96,376
Specific mass (kg/kW_e)	**3.53**	**6.43**

The main contributors to the disparity in masses for these two cases are the great differences in turbine/generator mass and reactor and shield mass. In considering why turbine/generator masses should be different, several factors may be considered. One is the need for vapor-

liquid separation equipment at one or more places in the turbine to keep the vapor quality in the turbine high. Another is the need for greater robustness in the Rankine turbine just because of the presence of liquid droplets when quality is less than unity. Third is the more conservative design algorithm in ALKASYSM as compared with that used in the GRC analyses. Turbine sizing is addressed in Appendix B.

The turbine mass, and therefore system overall specific mass, is highly sensitive to radiator temperature below 800 K, as will be discussed later. If we increased the radiator temperature on the Rankine system by 100 K, from 800 K to 900 K, the Rankine system specific mass drops to 4.94 kg/kW_e mostly as a result of turbine mass reduction. A further 100 K increase, to 1,000 K, increases specific mass to 5.03 kg/kW_e.

We now consider individual results for the two systems separately to show the effect of various parameter changes on the system specific mass.

Brayton Systems

Table 3 shows results for the Brayton power systems. Data in the upper part of the table are from the Glenn Research Center while data for reactor, shield, radiator, and total masses are from INEEL scaling.

Table 3. Results from Glenn Research Center and INEEL analysis of Brayton power systems.

Configuration (Table 1)	**UC2/NbC**	**UC2/NbC IHX**	**UC2/ZrC**	**UO2/SiC**	**UO2/ZrC**	**UN/Nb1Zr /Li**
Turbine inlet temperature (K)	1,640	1,640	1,920	1,520	2,100	1,350
Thermal Power (kW)	61579	61579	54283	61579	50614	75281
Compressor Pressure Ratio	2	2	2.2	2	2.3	1.9
Thermal efficiency (%)	24.4	24.4	27.6	24.4	29.6	19.9
Reactor mass (kg)	6,648	6,648	7,000	5,932	7,209	6,741
Shield mass (kg)	4,290	4,290	4,440	3,976	4,528	4,330
Heat exchanger mass (kg)	0	789	0	0	0	844
Turbine/generator mass (kg)	4,480	4,480	4,210	4,477	4,091	4,769
Main radiator area (m2)	5,563	5,563	3,294	7,639	2,502	11,232
Secondary radiator area (m2)	1,899	1,899	1,798	1,899	1,747	2,090
Total radiator mass (kg)	22,386	22,386	15,276	28,614	12,747	39,966
PMAD mass (kg)	15,106	15,106	15,106	15,106	15,106	15,106
Total mass (kg)	52,909	53,699	46,032	58,105	43,682	71,756
Specific Mass (kg/kWe)	**3.53**	**3.58**	**3.07**	**3.87**	**2.91**	**4.78**

In analyzing these data, it is no surprise that the configuration with the highest turbine inlet temperature (UO2/ZrC, 2100 K) has the lowest specific mass and vice versa. The worst specific mass shown is the one for which the reactor is cooled with lithium followed by a liquid-to-gas heat exchanger. It generates the most thermal power and has by far the largest radiator area because of the low temperature as well as the high power. Figure 3 shows graphically the relationship of the various mass components to turbine inlet temperature. Clearly, the greatest contributor to reduced system mass is reduction in radiator mass.

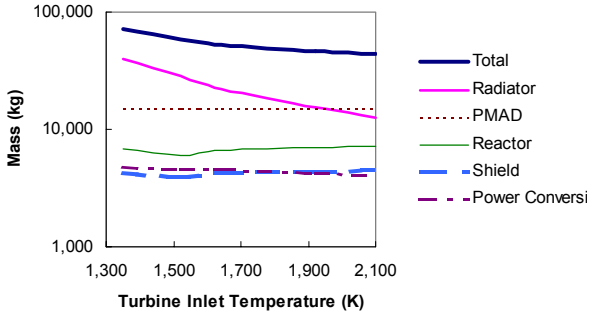

Figure 3. Brayton system specific mass decreases with increasing turbine inlet temperature.

Rankine Systems

A number of analyses were performed for Rankine systems. We begin with Table 4, which is similar to Table 3, showing corresponding data for the assumption of 800 K condensing temperature. Note that turbine inlet temperatures have been reduced to make the reactor outlet temperatures 1,350 and 1,500 K, respectively. We did not evaluate the UN/ASTAR 811C/Ga-Na case (gallium in the reactor and sodium as the working fluid) because, as is evident in Table 4, changing from lithium to gallium in the primary circuit and from potassium to sodium in the secondary each result in an increase of system specific mass

.

Table 4. Results for various Rankine cycle configurations assuming 800-K condenser temperature**.**

Configuration (Table 1)	**UN/Nb 1Zr/Li-K**	**UN/Nb 1Zr/Ga-K**	**UN/Nb 1Zr/Li-Na**	**UN/ASTAR 811C/Li-K**	**UN/ASTAR 811C/Ga-K**	**UN/ASTAR 811C/Li-Na**
Turbine inlet temp (K)	1,260	1,260	1,260	1,410	1,410	1,410
Thermal power (kWt)	59,108	59,108	62,026	49,819	49,819	49,436
Thermal efficiency (%)	25.4	25.4	24.2	30.1	30.1	30.3
Heat exchanger mass (kg)	2,254	3,296	1,205	868	960	493
PMAD mass (kg)	15,106	15,106	15,106	15,106	15,106	15,106
Main radiator area (m^2)	3,397	3,397	3,626	2,665	2,665	2,635
Secondary radiator area (m^2)	283	283	289	264	264	263
Radiator mass (kg)	11,039	11,039	11,746	8,789	8,789	8,696
Reactor mass (kg)	14,654	42,496	15,313	11,691	35,092	11,612
Shield mass (kg)	9,709	5,621	9,895	8,216	3,855	8,196
Turbine/Generator mass (kg)	43,614	43,614	292,801	57,820	57,820	468,938
Total mass (kg)	96,376	121,172	346,065	102,490	121,622	513,041
Specific Mass (kg/kW_e)	**6.43**	**8.08**	**23.07**	**6.83**	**8.11**	**34.20**

Several observations can be made from these data.

- Higher turbine inlet temperatures result in increases in system specific mass, even though reactor mass is reduced by about one fourth. That is due to greater turbine/ generator masses.
- Sodium as the working fluid in the Rankine system increases by about seven times the mass of the turbines but has little effect on reactor mass. The increased turbine size is due in part to the much greater specific volume of saturated sodium vapor than saturated potassium vapor at the same temperature, nominally by a factor of four. Liquid sodium also exhibits nominally twice the viscosity of liquid potassium, though it has a higher specific heat and thermal conductivity.

- Turbine/generator mass is dominant in all cases shown We examined cases where only two turbine/ generator units were assumed rather than four. Specific mass increased slightly with fewer units.
- Gallium in the primary circuit nominally triples the mass of the reactor over the lithium primary coolant case. Gallium has a lower thermal conductivity than lithium, implying larger areas for heat transfer, and it is an order of magnitude denser, which in itself will increase the reactor mass. It has a lower vapor pressure for a given temperature but a much lower specific heat, meaning higher mass flow rates to carry the required power.
- All of the concepts considered here are above the 5 kg/kW_e goal on the range of desired specific masses. However, they will be reduced if more optimistic values of turbine/ generator mass are used.

The temperature of the radiator and condenser has a strong influence on the system mass. Figure 4 shows how the various component masses vary as the temperature of the condenser is varied for Rankine-cycle cases where the reactor coolant exit temperature is 1,350 K. Similar behavior is seen in all of the other Rankine-cycle cases examined. Note that the ordinate is logarithmic. As earlier noted, changing the baseline assumption on condensing temperature from 800 to 900 K reduces system specific mass from 6.43 to 4.94 kg/kW_e for 1,350 K reactor exit temperature.

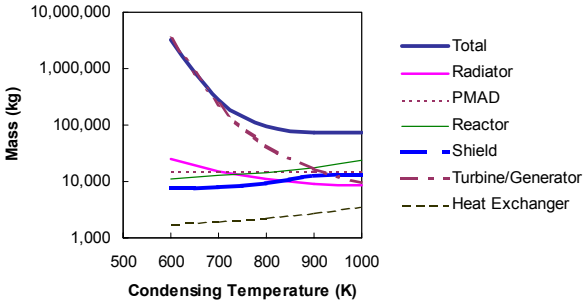

Figure 4 Variation in mass of Rankine system components with variations in condenser temperature.

We present a comparison of the effects of changing to an electric motor on the baseline and "growth" configurations for the lithium-cooled potassium option in Table 5. Assumed condenser temperature was 800 K. It will be seen there that the addition of the motor results in a slight increase in reactor mass. The difference in specific mass is less than 1 percent.

Table 5. Effects of changing from a vapor-driven turbine to an electric motor for feed pump power are minimal.

Configuration (Table 1)	**UN/Nb1Zr/Li-K Turbine**	**UN/Nb1Zr/Li-Na Electric Motor**	**UN/ASTAR 811C/Li-K Turbine**	**UN/ASTAR 811C/Li-K Electric Motor**
Turbine inlet temp (K)	1,260	1,260	1,410	1,410
Thermal power (kWt)	59,108	59,122	49,819	49,813
Thermal efficiency (%)	25.4	25.4	30.1	30.1
Heat exchanger mass (kg)	2,254	2,606	868	1,082
PMAD mass (kg)	15,106	15,106	15,106	15,106
Main radiator area (m^2)	3,397	3,402	2,665	2,745
Secondary radiator area (m^2)	283	283	264	264
Radiator mass (kg)	11,039	11,056	8,789	9,027
Reactor mass (kg)	14,654	14,657	11,691	11,690
Shield mass (kg)	9,709	9,710	8,216	8,216
Turbine/Generator mass (kg)	43,614	44,484	57,820	58,305
Total mass (kg)	96,376	97,619	102,490	103,426
Specific Mass (kg/kW_e)	**6.43**	**6.51**	**6.83**	**6.90**

A further comparison in Table 6 shows the effects of using direct boiling potassium in the reactors rather than a separate primary coolant, again for an assumed condensing temperature of 800 K. For the higher temperature case, specific mass is a little lower with direct boiling due to smaller turbine/generator mass. That, in turn, is due to the lower turbine-inlet temperature if the heat exchanger is present. Reactor mass is substantially increased for the 1,350-K coolant exit temperature while it is reduced for the 1,500-K case upon changing to direct boiling. That is due to the difference in reactor configuration produced by the design algorithm, and in particular, in the mass of the pressure vessel, which is much larger for the 1,350-K case. If condenser temperature were elevated to 900 K, the advanced performance fuel with direct boiling (last column) would have a specific mass of 3.94 kg/kW_e, mostly due to a reduction in turbine/generator mass.

Another point to be made here is that none of the Rankine system radiators as sized by the ALKASYS code would fit into the launch bay dimensions assumed. This was because of the large area of the radiators and the geometry assumptions built into the code. The launch-bay dimensions used, 23 ft diameter and 72.2 ft long, are for an advanced vehicle. The same problem would exist for the Brayton systems.

Table 6. Direct boiling of the working fluid gives marginally improved performance at higher temperatures.

Configuration (Table 1)	**UN/Nb1Zr/Li-K**	**UN/Nb1Zr/Li-Na Direct Boiling**	**UN/ASTAR 811C/Li-K**	**UN/ASTAR 811C/Li-K Direct Boiling**
Turbine inlet temp (K)	1,260	1,350	1,410	1,500
Thermal power (kWt)	59,108	52,577	49,819	45,945
Thermal efficiency (%)	25.4	28.5	30.1	32.7
Heat exchanger mass (kg)	2,254	0	868	0
PMAD mass (kg)	15,106	15,106	15,106	15,106
Main radiator area (m^2)	3,397	2,883	2,665	2,361
Secondary radiator area (m^2)	283	268	264	254
Radiator mass (kg)	11,039	9,453	8,789	7,846
Reactor mass (kg)	14,654	30,483	11,691	10,368
Shield mass (kg)	9,709	5,054	8,216	4,360
Turbine/Generator mass (kg)	43,614	39,229	57,820	53,239
Total mass (kg)	96,376	99,325	102,490	90,919
Specific Mass (kg/kW_e)	**6.43**	**6.62**	**6.83**	**6.06**

ADDITIONAL DATA

Here we provide specific data items requested by the sponsor, not previously given in this report.

Statepoint Schematics

Figure 5 shows a simplified flow sheet for the Brayton power system with mass flow rates and temperatures at key locations. Absolute pressures are somewhat arbitrary and depend on system sizing. Figure 6 is a corresponding schematic for the Rankine systems.

Key Failure Modes

- Unacceptable swelling of the reactor fuel
- Unacceptable release of fission products or spallation of cladding or coatings
- PMAD component failure due to radiation damage and/or high operating temperatures
- Turbine degradation by droplets or particulates
- Rotating machine bearing failure due to contamination or swelling.
- Loss of radiator capacity due to collisions by space debris

Key Component Lifetimes

Both reactor concepts are developmental. The NERVA/Rover reactor underwent extensive testing on developmental fuels, mostly for short periods, but there is limited testing using advanced high-temperature fuels or for long periods. There were some tests of SP-100 fuels at burn-ups appropriate for low power applications, but the reactor system was not tested. SP-100 fuel testing was not to sufficient burn-up levels for multi-megawatt power systems. Both Brayton and Rankine power conversion systems have had extensive industrial experience on earth, but neither has such experience in space. Radiator technology assumed here is based on heat pipes with expected performance based on engineering concepts and analyses with some experimental data. These, too, are very much developmental.

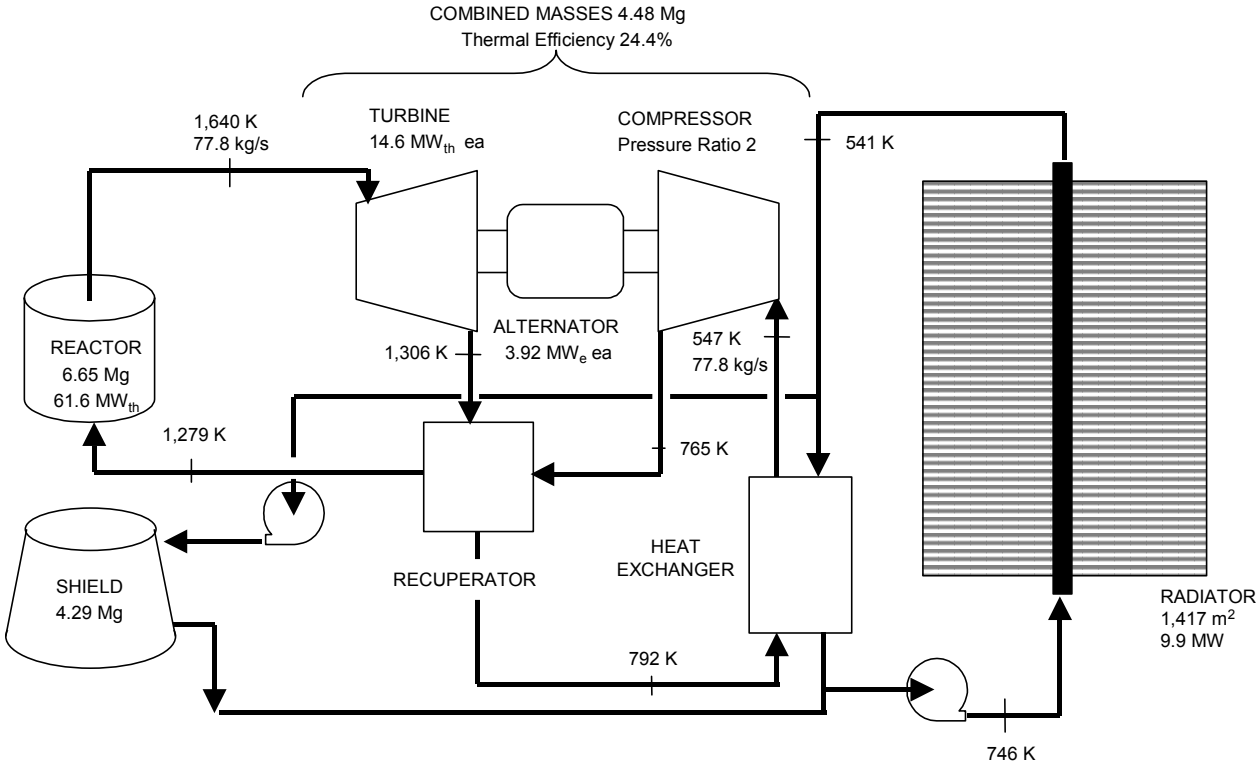

Figure 5. Simplified state-point diagram of the baseline Brayton power cycle system.

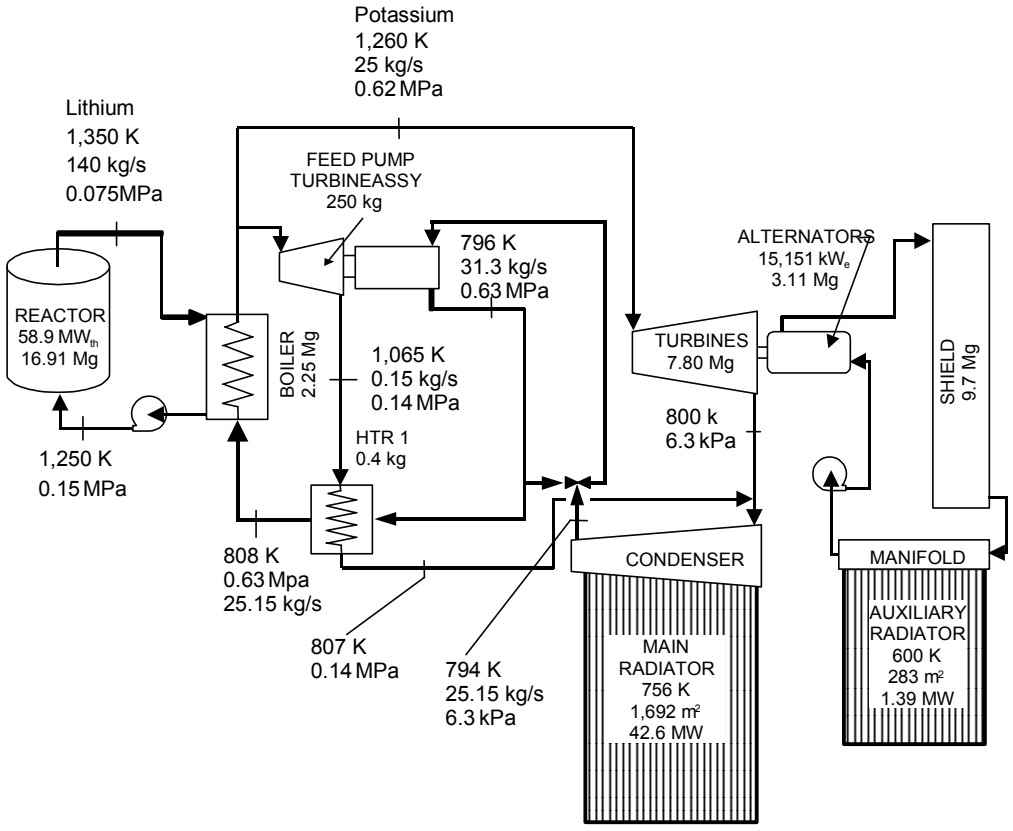

Figure 6. State-point diagram for baseline Rankine cycle system.

Evaluation Criteria

EC9 – Mission Operational and Design Lifetime

Both system classes considered in this trade study were intended to have a design operational lifetime of seven years.

Testing Program Requirements

Systems described are highly conceptual. Power conversion systems, because of their more extensive developmental experience, will require comparatively less ground testing than reactors and PMAD systems. However, confidence that power conversion systems would operate successfully in microgravity should be acquired. Reactor configurations and radiators will require extensive ground-based demonstration followed by verification of performance in microgravity, particularly for the liquid-cooled concepts. PMAD could be tested in environmental chambers. All key components should be evaluated for radiation resistance by irradiation of samples in a reactor and/or a high-field gamma facility.

EC10 – Materials Compatibility

Materials Utilized

Reactor fuel materials may be UN, UC_2, or UO_2 with claddings or coatings as described in Table 1. Reactor structures may be of Nb-1Zr or ASTAR 811C for liquid-cooled reactors and possibly carbides (NbC, ZrC, or SiC) for the gas reactors. Turbine materials are not yet specified for either system, but the high-temperature materials needed for the gas systems proposed will probably have to be a ceramic or cermet. Advanced semiconductor materials such as doped diamond films may be needed for PMAD, and circuit boards will probably have to be ceramic to withstand the irradiation and the temperatures. Superconducting materials for motors, generators, and distribution systems may be considered.

Compatibility Issues

Materials compatibility will have to be verified for many of the structures and components. Compatibility at high temperatures and in a radiation field is largely unexplored. Particular issues include

- Metallurgical stability of structural materials exposed to hot alkali metals
- Erosion of turbine blades by hot alkali metals
- Radiation-induced decomposition of materials at high temperatures
- Dielectric breakdown of insulators from radiation effects and material migration

EC11 – Reliability

Few of the components considered in systems such as the ones described here have established reliability data bases under the conditions proposed for use. There will not be the luxury of time to develop such reliability data bases if a mission in the next decade is contemplated. Rather, reliability inference based on analytical methods and sparse data sets will be required.

Failure Modes and Effects Analysis

Detailed failure modes and effects analysis of any of these systems is premature at this point because of the lack of design detail.

Shield Design

Estimated shield masses have been provided in the comparison data. The shield design for the Rankine systems is a composite of tungsten for gamma suppression and a mixture of lithium hydride and stainless steel for neutron suppression and capture. The ALKASYSM code generates thicknesses and sizes needed to protect to a specified level over a specified plane. For the NERVA Derivative design, shielding is a mixture of borated aluminum and titanium hydride.

Radiation Fields

The shielding criteria for this study were gamma dose less than 5×10^5 rad and neutron fluence (1-MeV equivalent) less than 1×10^{13} n/cm^2 over the seven year operating life at a location 22.5 m distant from the reactor core. These limits are adequate to protect currently available instruments and electronics. They are not sufficient for biological protection. Use of advanced, radiation-hardened components may allow the relaxation of the shielding criteria, implying higher radiation fields could be tolerated. Components operating much closer to the shield or on the reactor side of the shield will see much more intense radiation fields. Thermal radiation to the rest of the spacecraft from the radiator panels cannot be neglected nor can natural background radiation from space.

Mitigating Design Features

The on-board control system will need to be adaptive to compensate for such effects as shifts in reactor reactivity, loss of radiator capacity due to debris impact, failure of one of the power conversion systems, and varying solar insolation. Further, operation at varying load during different phases of the mission will be required. Specifics have not yet been determined due to the preliminary nature of the designs.

EC16 – Technical Maturity and Development Requirements

Test, Demonstration, and Application Histories

As previously stated, the reactor designs used as a basis for this trade study were based on SP-100 designs for the liquid-cooled concepts and on the Enabler NERVA Derivative design for gas-cooled reactors. While there was considerable testing of the NERVA concept as a nuclear thermal rocket, the SP-100 was designed and analyzed but never really tested. Both Brayton and Rankine power conversion systems have extensive terrestrial application histories, but neither has space demonstration sufficient to establish credibility, particularly for the power levels addressed here. Higher temperature operation will be needed than has previously been demonstrated. PMAD systems using available components are limited to operating temperatures less than 450 K. Higher operating temperatures will be needed to minimize radiator masses and thus meet system specific mass goals. Superconducting electrical components have been under development for some time, and there is

confidence in their ultimate availability. Insulation and heat removal techniques required for achieving superconducting temperatures in or adjacent to a hot power system require further work.

Technical Readiness (TBD)

Principal R&D Requirements (TBD)

Required Test Facilities

Replication of radiation, vacuum, and temperature environments for ground testing should be addressed early. A key issue is the degree to which radiation and other environments can be separated for ground testing. For systems requiring two-phase flows, the effects of microgravity could be substantial, and effort should be applied to finding innovative ways to evaluate heat transfer in two-phase fluids under weightless conditions.

Existing Domestic Facilities

The Advanced Test Reactor (ATR) at the INEEL has sufficient flux and test volume to perform meaningful neutron irradiation experiments on components is.[14] Gamma irradiation facilities are also available at ATR. The High Flux Isotope Reactor (HFIR) at Oak Ridge National Laboratory also has some capability for such irradiations. Evaluation of heat transfer and fluid management for two-phase flows may be best done on the International Space Station, though experiments on shuttle missions could also be valuable. Large thermal and vacuum facilities exist at various NASA sites, GRC in particular. Ground testing of an integrated reactor and power conversion system could be performed at the Contained Test Facility at the INEEL.

Existing International Facilities

Foreign reactor facilities with reasonably large neutron fluxes and test volumes include the BR-2 reactor in Belgium, the High Flux Experimental Test Reactor (HFETR) in China, and the MIR-M1 and SM-2 reactors in Russia.

Environmental and Health/Safety Issues

A dominant concern is minimization of radiological risk associated with launch accidents and ultimate disposal of the reactor and associated components. One proposed approach to minimizing the launch risk is to assemble the reactor in earth orbit and only initiate criticality then. That has considerable technological and cost risk that may be mitigated by assembling the reactor on earth and bringing it to criticality but at negligible power before launch.

Once the system has completed its useful life, possibly after several missions, the issue is whether to bring it back to earth intact, or to dispose of it in space. Complete destruction with wide dispersal into the earth's atmosphere is not considered a viable option.

CONCLUSIONS

The analyses conducted in this trade study have compared specific masses for various configurations of both gas-cooled reactors with Brayton cycle power conversion systems and liquid-cooled reactors having Rankine cycle power systems. The methodology employed took advantage of existing models for estimating some component masses for the respective systems. Reactor and shield masses for the liquid metal systems were generated by the ALKASYSM code while those of the gas reactor systems were scaled from Enabler NERVA Derivative reactor values.

While the Brayton power system option appears to have the specific mass advantage, both systems have the potential to approach the 3–5 kg/kW_e specific mass objective of the MMW program. The main contributing factors for the apparent gas-Brayton advantage are the higher operating temperatures for gas-cooled Brayton systems and the optimistic values for turbine/ generator masses compared with the more pessimistic values determined by the ALKASYSM code for the Rankine systems.

We explored variations in system configuration including changing fluids and replacing the feed pump turbine in the Rankine configuration with an electric motor. Substituting

electric motor driven feed pumps for turbine driven pumps slightly increased (less than 1 percent) system specific masses. Using direct boiling potassium instead of liquid lithium offered a small (11 percent) reductions in specific mass for the higher temperature configuration, but it increased the mass of the low-temperature design because of much higher reactor mass. Neither substituting gallium for lithium nor sodium potassium offered any improvement in Rankine system specific mass. Quite the contrary, specific masses increased markedly in each case. Increasing condensing temperature from 800 to 900 K had a marginal effect in reducing system specific mass for Rankine systems except for the advanced technology direct boiling case where a 50% improvement was seen. Going to lower condensing temperature drastically increased system specific mass.

One of the key issues relates to practical limits on radiator temperature. Another technological concern is the areal density of radiators and the ability to fit the large radiators required for this power level into launch vehicles. Turbine/generator mass is also an area of uncertainty that requires further resolution.

REFERENCES

1. E. J. Wahlquist, DOE-NE-50, Memorandum to Warren Bergholz, DOE-ID, December 2000.

2 . F. R. Chang-Díaz et al., "The Physics and Engineering of the VASIMR Engine," AIAA 2000-3756, 36th AIAA/ASME/SAE/ASEE Joint Propulsion Conference, Huntsville, AL, July 17-19, 2000.

3. J. Wheeler, DOE-NE-50, Memorandum to SNL/LANL and INEEL Concept Teams, "Supplemental Guidance for SPFT Concept Definition Effort," February 20, 2001.

4. Special Purpose Fission Technology Program, *Design Data Request for: Surface Power and Nuclear Electric Propulsion Power Systems*, ORNL/SPFT/LTR-001, Rev. 1, February 9, 2001, Oak Ridge National Laboratory.

5. L. L. Rutger and V. C. Truscello, The SP-100 Power System," *AIP Conference Proceedings No. 246*, 1992, American Institute of Physics.

6. B. L. Pierce, "Application of the Enabler to Nuclear Electric Propulsion," *Proceedings, Eight Symposium on Space Nuclear Power Systems, Albuquerque, NM, January 6-10, 1991, Part One*, pp. 379-384.

7. J. C. Moyers and J. P. Nichols, *ALKASYS, a Computer Program for Studies of Rankine-Cycle Space Nuclear Power Systems*, ORNL/TM-10427, September 1987, Oak Ridge National Laboratory.

8. G. R. Longhurst. "ALKASYS Code Adaptation," INEL/EXT-01-00539, April 2001, Idaho National Engineering and Environmental Laboratory.

9. L. S. Mason, NASA Glenn Research Center, private communication, March 21, 2001.

10. W. W. Engle, Jr., et al., *Optimization of a Shield for a Heat-Pipe-cooled Fast Reactor Designed as a Nuclear Electric Space Power Plant*, ORNL/TM-3499, June 15, 1971, Oak Ridge National Laboratory.

11. R. A. Robinson et al., *Brayton-Cycle Radioisotope Heat Source Design Study: Phase I (Conceptual Design) Report*, ORNL/TM-1691 (NASA CR-72090), pp. 90-100, December 1996, Oak Ridge National Laboratory.

12. D. E. Carlson, *A Parameter Study for the SP-100 Radiation Shield*, SP TN 101, 1985, Los Alamos National Laboratory.

13. M. P. Moriarity and W. R. Determan, "SP-100 Advanced Radiator Designs for Thermoelectric and Stirling Applications," *Proceedings of the 24th Intersociety Energy Conversion Engineering Conference, Washington, DC, Aug. 6-11, 1989*, IEEE CH2781-3/89, pp. 1245-1250.

14. A. G. Ware and G. R. Longhurst, *Test Program Element II Blanket and Shield Thermal Hydraulic and Thermomechanical Testing, Experimental Facility Survey*, EGG-FT-5626, December 1981, Idaho National Engineering and Environmental Laboratory.

APPENDIX A

RADIATOR AREAL DENSITY

INTRODUCTION

After examining the output from the ALKASYSM code and reviewing the data from the Glenn Research Center, an independent estimate for the radiator configuration was desired. This appendix explains the procedure used to determine the areal density for an independent heat pipe radiator design.

Areal density is the ratio of the heat pipe radiator system total mass to the radiating area. Providing a minimal areal density is accomplished through an optimization of heat pipe characteristics. The most desirable design consists of the lightest, most durable pipe that can transport the most heat. Variable parameters considered were pipe wicking materials, pipe materials, pipe size, operating temperature, and heat output.

For an optimal wicking material and design, a wick of low density and high capillary capabilities was considered ideal. Wick designs considered included wire mesh, sintered powder, and carbon fiber artery. Copper, having a high thermal conductivity, was selected as the wick for both wire mesh and sintered powder wicks. Because thermal conductivity was not a primary concern for the arterial pipe and because it is consistent with the composition of the heat pipe, carbon-carbon fiber was chosen for the arterial wick.

AXIAL TRANSPORT LIMITATIONS

There are inherent physical limitations to heat pipe performance in terms of the heat that can be transported axially in the pipe. A comparison of axial limitations to performance of various heat pipe configurations appears in Figures A-1 to A-3. The limits illustrated by the graphs include sonic, capillary, entrainment, and boiling. Acceptable design regions lie below the lines shown.

Sonic Limit

The sonic limit is the choking of the flow as it passes through the barrel of a heat pipe. Flows cannot exceed the speed of sound in a duct of constant cross sectional area. As the vapor velocity approaches the speed of sound, a temperature drop in the condenser will occur, which will limit the capability of the pipe to radiate heat. Thus, Levy's equation is used to determine the power level at which the vapor in a heat pipe approaches sonic velocity.[A1]

Capillary Limit

The capillary limit describes the bound in the capability of the wick to return the fluid to the evaporator. If the fluid cannot return to the evaporator quickly enough, the pipe evaporator or boiler will dry out, and heat pump functioning will cease.

Entrainment Limit

Entrainment in a heat pipe occurs when Bernoulli and viscous drag forces remove the liquid from the wick and it is carried by the vapor flow. This limitation is based on the vapor velocity and characteristics of the liquid-vapor interface. If entrainment occurs, the wick dries out.[A2]

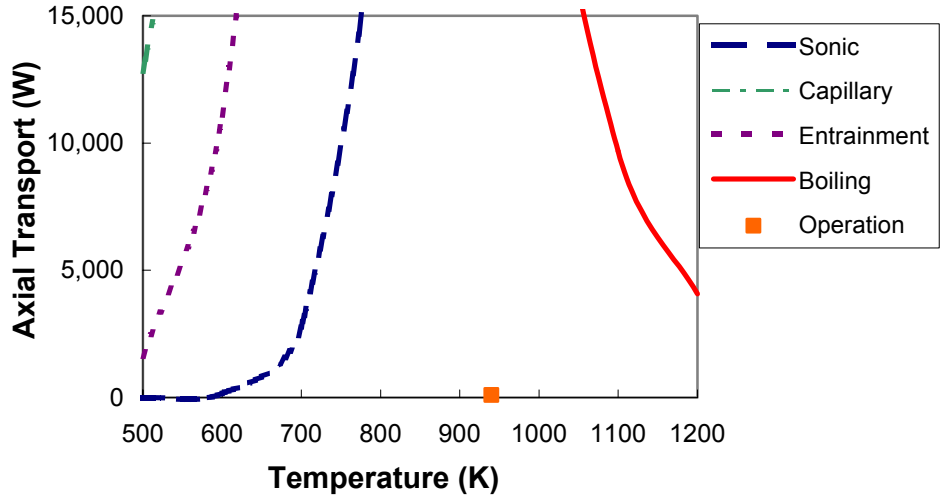

Figure A-1. Axial limitations for a sintered powder wick.

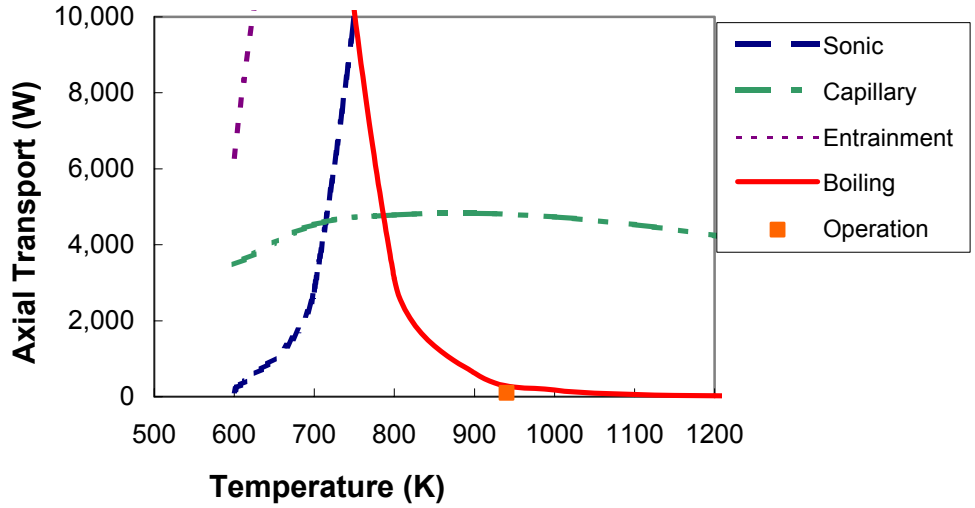

Figure A-2. Axial limitations for a carbon fiber artery wick.

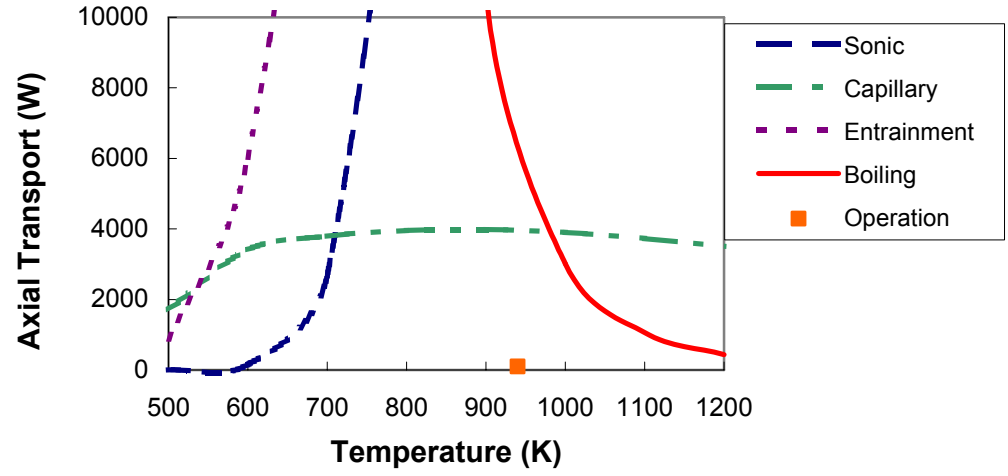

Figure A-3. Axial limitations for a wire mesh wick.

Boiling Limit

Boiling in the wick depends on the liquid-vapor interface, and the wetting characteristics of the wick material. This limitation affects the radial heat transport capability of the wick in the evaporator. If film boiling develops, heat transfer is greatly reduced, and the heat pipe performance is diminished.[A3]

Figures A-1 to A-3 indicate that the sintered powder wick offers the most feasibility with respect to axial limitations; however, the arterial wick is capable of operating within the specified range at a lower mass. Thus, the arterial wick was chosen based on its mass.

PIPE MATERIAL SELECTION

Pipe material selection was based on a high strength-to-mass ratio, since a lightweight, durable pipe is desired. The SP-100 design specifies carbon-carbon fiber construction, which is lighter than comparable stainless steel construction.[A4] Selection of carbon-carbon fiber for the present work was based on this design.

PIPE SIZE AND OPERATING TEMPERATURE

Pipe size and operating temperature were obtained from a system of heat transport equations[3] that were constrained by total pipe length, heat output, exchanger temperature, and heat exchanger convective coefficient. Heat pipe temperature is found from an equation for the radiation heat exchange over the cylindrical area for a given pipe,

$$\frac{T_p - T_\infty}{Q} = \frac{1}{\rho\sigma 2\pi \Im r L_2 T_p{}^3} \qquad \text{(A-1)}$$

where

T_p = pipe temperature

T_∞ = space temperature

Q = pipe heat output

ρ = carbon-carbon fiber density

σ = Stefan-Boltzmann constant

$\Im$ = pipe view factor

r = pipe outer radius

L_2 = pipe length at condenser.

We assume T_∞ is effectively 0 for the region seen by the surface corresponding to empty space and T_∞ is identically T_p elsewhere, that $\Im = 0.4$ is the view factor to empty space rather than other radiator surface. Solving for T_p yields

$$T_p = \left(\frac{Q}{\rho\sigma 2\pi \Im r L_2} \right)^{1/4} \qquad \text{(A-2)}$$

The length of the heat pipe evaporator in the heat exchanger is obtained from a convection equation

$$\frac{T_o - T_p}{Q} = \frac{1}{L_1 r h_c 2\pi} \qquad \text{(A-3)}$$

where

L_1 = pipe evaporator length

h_c = heat exchanger convection constant.

Solving for L_1 yields

$$L_1 = \frac{Q}{(T_o - T_p) r h_c 2\pi} \qquad \text{(A-4)}$$

Constrained by a total length, L_T, the length L_2 of the pipe in the radiating condenser must be

$$L_2 = L_T - L_1 \qquad \text{(A-5)}$$

An equation for r can be obtained from the equation governing the heat transport across the pipe, including evaporation, transport, condensation[A5], and radiation processes:

$$\frac{T_o}{Q} = \frac{1}{r2\pi} \left(\frac{1}{L_1 h_c} + \frac{1}{\rho \Im \sigma L_2 T_3{}^3} \right) \qquad \text{(A-6)}$$

[a] Evaporation, transport, and condensation within the heat pipe were assumed to occur at constant temperature.

Solving for r yields

$$r = \frac{Q}{T_o 2\pi}\left(\frac{1}{L_1 h_c} + \frac{1}{\rho \Im \sigma L_2 T_3^{\,3}}\right) \qquad \text{(A-7)}$$

From Equations (A-2), (A-4), (A-5) and (A-7), values of T_p, L_1, L_2, and r can be determined.

We iterated over a range of values for h_c, T_o, Q, and L_T. for heat pipe size optimization. A baseline was developed and compared with results obtained by making changes to one parameter at a time. Changing T_o and h_c caused decreases in the total radiating surface area, whereas changes in Q and L_T effected changes in pipe number and radius. However, none of these parameter changes had any effect on areal density. Figures A-4 and A-5 illustrate trends in the radiator area based on variations in the input parameters.

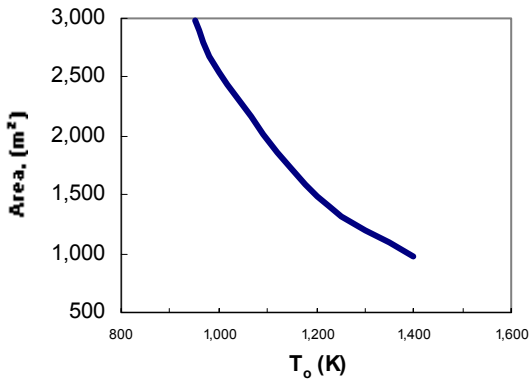

Figure A-4. Increasing T_o decreases radiating area.

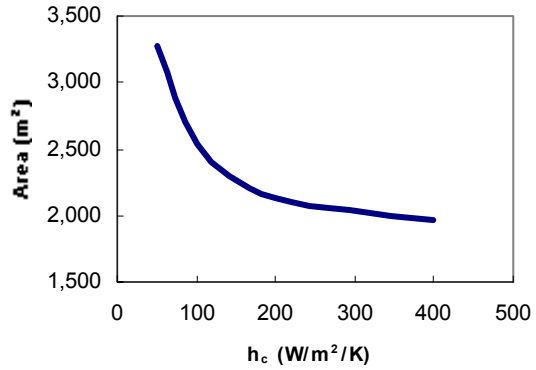

Figure A-5. Increasing h_c decreases area.

It should be noted that the area referred to in Figures A-4 and A-5 is the projected area of all the pipes, and not of the entire system, which has spaces between the pipes.

HEAT EXCHANGER

The heat pipe radiator system includes an elliptical heat exchanger, with major outer axis of 12.1 cm, minor outer axis of 4.1 cm, and 1mm thickness, as in Figure A-6. This heat exchanger was assumed to work with condensing potassium. The liquid potassium volume fraction of the heat exchanger was assumed to be one-sixth.

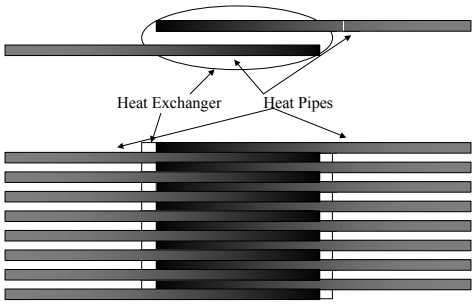

Figure A-6. Heat pipe heat exchanger schematic.

Improvements may be made to the heat exchanger design to yield a higher coefficient of convection and a smaller mass. These changes would result in a lighter radiator with less area.

Fin inclusion was studied, but results were unclear as to whether fins improved the areal density and/or total area. Inclusion of an efficient fin design may significantly improve the capabilities of both the radiator and the heat exchanger.

For the purposes of this calculation, a total plenum length of 5,320m was considered. This system will be challenging to fit into a Space Transportation System launch bay.

RESULTS AND DISCUSSION

As shown in Table A-1, a final areal density of 5.05 kg/m^2 was attained, which can operate 400,000 pipes with each pipe at 100 watts. This is not necessarily the configuration that would be built, because the number of heat pipes is excessive, but it represents the optimal configuration for radiator system mass. The coefficient of convection in the heat exchanger is expected to be 200 W/m^2/K. The heat exchanger is designed to operate at 1000 K, while the pipe will operate at 940 K. Uncertainties and possible improvements include heat exchanger properties and design, fin inclusion, and radiator configuration.

We should add that this parametric study is far from complete design. There will yet be considerable design effort required to address such things as pumps and phase separators for liquid phase fluid transport. Those components would add to the system mass.

Table A-1. Optimal design parameters for independent heat pipe design.

Heat Pipe Properties					
Diameter			Length		
Outer	1.33E+00	cm	Condenser	2.00E-01	m
Inner	8.33E-01	cm	Evaporator	2.00E-01	m
			Total	4.00E-01	m
Mass					
	1.40E-02	kg			

Interior Properties					
Wick			Vapor Core		
Fluid Flow Cross Secti	2.53E-06	m^2	Sodium Vapor Dens	5.32E-03	kg/m^3
Na-Fluid Density	8.74E+02	kg/m^3	Cross Section	1.26E-03	m^2
Na-Fluid Volume	1.01E-06	m^3	Mass	2.68E-06	kg
Mass	1.16E-09	kg			

System Properties					
Pipes			Heat Exchanger		
Number Of	4.00E+05		Shell Mass	4520	kg
Total Pipe Mass	1.40E-02	kg	Potassium Mass	5970	kg
Pipe System Mass	5.62E+03	kg			
			Total		
			Mass	1.61E+04	kg
			Area	3.19E+03	m^2
			Areal Density	5.05E+00	kg/m^2

APPENDIX A REFERENCES

A1. S. W Chi, *Heat Pipe Theory And Practice: A Sourcebook*, Washington, D.C.: Hemisphere Publishing Company, 1976, pp. 79-82.

A2. Chi, *Heat Pipe*, 86.

A3. Chi, *Heat Pipe,* 89-90.

A4. M. P. Moriarty, and W. R. Determan, "SP-100 Advanced Radiator Designs for Thermoelectric and Stirling Applications," *24th Proceedings of the IECEC,* New York: Society of Automotive Engineers, 1989, pp. 1245-1250.

A5. A. F. Mills, *Heat Transfer*, Upper Saddle River: Prentice Hall;1999, pp. 77-79.

APPENDIX B

TURBINE MASS ESTIMATES

COMPARISON WITH COMMERCIAL DESIGNS

To examine the realism of the turbine mass estimates, we compared the turbine/generator masses predicted by the GRC Brayton model and by the ALKASYSM code with data from General Electric Power Systems' large commercial turbine/generator sets.[B1] The resulting plot is shown in Figure B-1. The masses given in the GE data are for complete open cycle Brayton systems including turbines, generators, housings and structural supports, sitting on a pad. The log-linear fit shown gives a mass at 15 MW_e of 108,961 kg, while the mass predicted by ALKASYSM for condensing temperature of 800 K is 47,194 kg. The mass predicted by the Brayton model is 4,480 kg, substantially below either of those values.

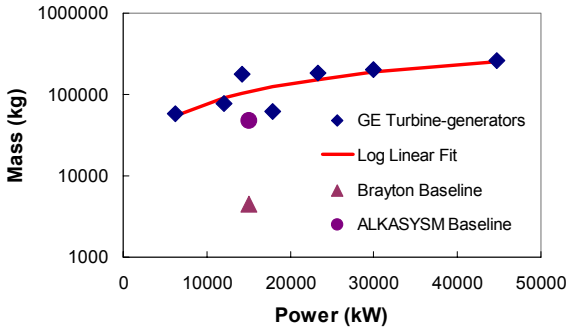

Figure B-1. Comparison of commercial turbine masses with those predicted by the Glenn Research Center model and by ALKASYSM for baseline cases.

A further datum for comparison is an estimate made by Morgan et al.[B2] that a 10-MW Brayton power conversion system would have a mass of about 25,800 kg. The fit in Figure 3 gives 79,505 kg for 10 MW_e, more than three times the value of Morgan et al. The estimate of Morgan et al. for a liquid-metal power conversion system is 33 percent larger than for a Brayton system. Therefore, it may be that the turbine mass model in the Brayton calculations is for a much more advanced system.

The turbine/generator mass values of Morgan et al. scaled using the log-linear slope of Figure B-1 to 15 MW_e, are 35,359 kg for the Brayton system and 47,008 kg for the Rankine system. The latter number is surprisingly close to the ALKASYSM prediction of 43,614 kg. If we used the 35,359-kg value for the baseline Brayton system, the overall specific mass would increase from 3.53 to 5.59 kg/kW_e.

TURBINE/GENERATOR MASS ALGORITHMS

Here are compared two algorithms for estimating turbine masses for Rankine cycle power systems. The first is that used in the ALKASYS-PC code[B3], while the second is the methodology of S. L. Hudson[B4]. In each case, the objective is to use relatively simple formulas and parameters to estimate the mass of a turbine system given such things as working fluid states and required power.

ALKASYS-PC

The general algorithm used in the ALKASYS-PC code is to define turbine inlet and exit conditions, the enthalpy change in the last stage by the limiting blade tip velocity, the total number of stages required for total power output under the assumption of nominally equal enthalpy drops per stage, and then to assume equal temperature drops per stage to estimate thermodynamic states and thereby detailed flow parameters at each stage. This is done first on a unit-mass basis, and then the turbine is sized based on the mass flow required to generate the specified power. These are now examined in detail.

First the entry conditions for the working fluid are defined. This is specified by the boiler or reactor exit temperature T_{boil} and the vapor quality x_{boil} at the boiler exit. A subroutine for

thermodynamic properties (line 6000) then calculates

P_o = saturation pressure (atm)

v_{f_o}, v_{g_o} = specific volume (ft^3lbm) for liquid and vapor phases[a]

h_{f_o}, h_{g_o}, h_{fg_o} = enthalpy (BTU/lbm) for liquid, vapor, and transition

s_{f_o}, s_{g_o}, s_{fg_o} = entropy (BTU/lbm °R) for liquid, vapor, and transition

for the turbine inlet point. Using the specified quality, the working fluid specific volume v_o, enthalpy h_o, and entropy s_o at the turbine inlet are then found.

$$v_o = v_{f_o} + x_{boil}\left(v_{g_o} - v_{f_o}\right) \quad \text{(B-1)}$$

$$h_o = h_{f_o} + x_{boil}\, h_{fg_o} \quad \text{(B-2)}$$

$$s_o = s_{f_o} + x_{boil}\, s_{fg_o} \quad \text{(B-3)}$$

Temperature is then changed to the condensing temperature, T_{con}, and the subroutine then calculates the same properties for the turbine exit point.

P_n = saturation pressure (atm)

v_{f_n}, v_{g_n} = specific volume (ft^3lbm) for liquid and vapor phases

h_{f_n}, h_{g_n}, h_{fg_n} = enthalpy (BTU/lbm) for liquid, vapor, and transition

s_{f_n}, s_{g_n}, s_{fg_n} = entropy (BTU/lbm °R) for liquid, vapor, and transition

Using the assumption that the turbine is adiabatic and reversible, the exit vapor quality is then estimated from

$$x_n = \frac{s_o - s_{f_n}}{s_{fg_n}} \quad \text{(B-4)}$$

and then

$$h_n = h_{f_n} + x_n\, h_{fg_n} \quad \text{(B-5)}$$

To compute the enthalpy drop in the last stage, the assumption is made that the turbine blades have the same length as the hub radius at each stage and that the last stage blade tip velocity v_{tip} is specified in the input. A further assumption is made that the ratio of the spouting velocity (circumferential component of total jet velocity) to the blade circumferential velocity is 2 at the blade midpoint to maximize impulse efficiency. Then with the further assumption of 50 percent reaction in turbine stage design, the enthalpy decrease in the nozzle of the last stage is found from first law analysis

$$L\left(\frac{BTU}{lbm}\right) = \frac{\left(1.5\, v_{tip}\right)^2}{2\, g_c} \quad \text{(B-6)}$$

The parameter $g_c = 32.174\left(\frac{ft\ lbm}{lbf\ s^2}\right)$ is the units commensuration constant for masses in the English units system. The implementation in the code is

```
90 L = 2.25 * VTIP ^ 2 / 50103! -
1.25
```

and we assume that the 1.25 (BTU/lbm) (2.905 J/g) reduction is for the inefficiency of the nozzle. "To account for the fact that the enthalpy drop is greater for the last stage than for the average stage in a turbine having equal temperature drops across all of the stages, the number of stages is then set equal to the integer nearest to 1.1 times the isentropic enthalpy difference between turbine inlet and condenser temperatures divided by the last stage enthalpy drop."[3] In equation form,

$$n = \mathrm{CINT}\left(\frac{h_o - h_n}{L}\right) \quad \text{(B-7)}$$

An external moisture separator is assumed to be placed at about the middle stage. It is assumed to remove 90 percent of the liquid and 0.1 lbm of vapor for each lbm (0.1 kg/kg) of

[a] The ALKASYS-PC code uses mostly English units.

liquid removed and to result in a 1.5 psi (10.3 kPa) pressure drop in the fluid. An interstage separator is assumed at the next to last stage. It is assumed to remove 25% of the moisture entering it and 0.25 lbm of vapor for each lbm (0.25 kg/kg) of liquid removed.

Temperatures between each of the stages are then found by interpolation assuming the same temperature drop per stage. Fluid pressure, enthalpy, vapor quality, and specific volumes are computed at the stage exit from the assumption of isentropic expansion. Stage thermodynamic efficiency is assumed to be a common input value degraded by one percentage point for each percent of moisture in the fluid stream. Mass flow rates through the various stages are reduced by flows taken to the moisture separators. An enthalpy loss is also attributed to the exit momentum of the fluid from the turbine, the value of which is an input to the problem.

With actual enthalpy change through the various stages calculated on a unit-mass basis, the mass flow required to develop the specified power level in the turbine is found.

$$\dot{m}\left(\frac{\text{lbm}}{\text{s}}\right) = 0.9479\,\frac{\dot{W}_{gen}}{\dot{w}_{turb}\,\eta_{gen}} \qquad \text{(B-8)}$$

turbine, and η_{gen} is the electrical efficiency of the generator/alternator.

Using the mass flow and the fluid specific volume at the exit, the exit volumetric flow rate Q_{LS} is found. Then with an assumed nozzle angle of 14° and the hub to tip radius ratio of 0.5, the required flow area and hence the exit blade tip diameter may be found.

$$D_{tip}\ (\text{in}) = \left(\frac{192}{3\pi}\right)\left(\frac{2\,Q_{LS}}{3\,\tan(14^\circ)\,v_{tip}}\right)^{1/2} \qquad \text{(B-9)}$$

where $\dot{W}_{gen}$ is the electrical power in kW delivered by the generator, $\dot{w}_{turb}$ .is the work (BTU/lbm) done by the working fluid on the Turbine inlet blade tip diameter is arbitrarily assumed to be half that value. An arbitrary turbine shell thickness of 2.5 inches (6.35 cm) is assumed.

Turbine length is assumed to be made up of 5 components: the stage lengths, bearing lengths, inlet and exit manifold lengths, length due to moisture separators, and the shell thickness of 5 inches (12.7 cm). Empirical fits for these are combined into

$$L_{turb}\ (\text{in}) = 5 + (0.84 + 0.4\,n)\,\dot{W}_{gen}^{0.25} + \frac{Q_{LS}}{D_{tip}} \qquad \text{(B-10)}$$

The resulting volume is a conic frustum whose mass is estimated based on a superficial density, which consists of a metal density and solidity. Table B-1 lists the values for the two materials assumed in the code.The transition to ASTAR-811C is assumed to take place at a predetermined turbine inlet temperature, typically 1,400 K.

Alternator mass is calculated in a similar fashion. Alternator rotor angular speed is set by the turbine blade diameter and tip velocity. Alternator diameter is then set by the design stress level for rotor failure, assumed to be 406,000 psi (276 MPa) with an assumed material density for steel. Alternator length is obtained from an empirical fit to electric power and alternator diameter. Finally, again using a superficial density and a right circular cylindrical shape, the alternator mass is calculated from the length and diameter.

Changes in the calculated masses of the turbine and alternator can be brought about by making changes in the assumptions. One that

Table B-1. Density values used in the ALKASYS-PC code for calculating turbine masses.

Material	Metal Density (lb/in^3)	Solidity	Superficial Density (lbm/in^3)
TZM Alloy	0.360	0.34	0.123
ASTAR-811C	0.604	0.34	0.207

may be straightforward is the assumption of a higher strength alloy for the alternator rotor. Thinner turbine casing also may be possible. Increasing low-pressure-end blade tip speed is another option.

Hudson Model

The Hudson model[B4] has many similarities to the ALKASYS-PC model, but there are some important differences as well. The Hudson model

> determines the blade length and disk radius for each stage of a turbine by calculating: (1) the energy transfer from the working fluid to the rotating blades for each stage of the turbine; (2) the flow area required by the working fluid as it exits each stage; and (3) the limiting stage blade speed due to material strength considerations. The process is iterative because of the interdependence of these calculations. Blade length and disk radius are then used to define the turbine stage size because they are the primary limiting dimensions.[B4]

Though conducted in a different sequence, many of the calculations in this model are similar to those in the ALKASYS-PC model regarding power per stage and flow areas required, but it is difficult to tell if it is more or less sophisticated regarding changing vapor qualities and the presence of liquid separators.

Rather than use last stage blade tip speed as a predetermined parameter, the Hudson model determines the maximum rotational speed allowed to maintain stresses in the blade root and disk stresses in the hub at acceptable levels. Blade stress σ_b is found from

$$\sigma_b = \rho_b \; 0.7 \; N^2 \; R_m \; L \qquad \text{(B-11)}$$

where ρ_b is the density of the blade material, N is the angular rate (radians/s) of the blade, R_m is the blade mean radius, and L is the disk length, all in commensurate units. The factor of 0.7 accounts for tapered blades. Maximum disk radius R_d is set by the allowed stresses

$$R_d = \frac{\sqrt{\frac{\sigma_d}{0.9 \; \rho_d}}}{N} \qquad \text{(B-12)}$$

where σ_d is the allowed stress in the disk and ρ_d is the density of the disk material

For estimates of turbine mass,

> The overall turbine volume and mass is the sum of the individual stage volumes and mass. Stage volumes are obtained by multiplying the cross-sectional area of each stage (disk and blade swept areas) by the stage thickness, which is determined from a specified aspect ratio (the ratio of the blade length to blade axial thickness). The individual stage volumes include the disk, blade, and nozzle volumes. The turbine blade swept volume and nozzle volume is then given a mass based on an average density 30% that of the blade material density. The disk volume (the circular disk area without deduction for the shaft center bore times the blade axial thickness) is assigned an average density 100% that of the disk material density. The remaining stage volume between disks is provided a mass based on 20% of the disk material density to account for seals, shaft and connections. The casing mass is determined from hoop stress calculations and the resultant disk material required thickness. Although no specific mass is allotted for some turbine mechanical components such as bearings, ducting, seals, and cooling passages, the gross density estimates indicated above are intended to account for them in providing the overall turbine mass.[B4]

Comparison

Figure B-1 shows the results of a parametric study performed by Hudson[B4] with corresponding results from ALKASYSM, the modified ALKASYS-PC code used in our comparison studies. In each case, it was assumed that the working fluid was potassium, that the turbine inlet temperature was 1350 K, and that the inlet pressure was the saturation pressure. Turbine outlet temperatures ranged from 900–1,200 K for the Hudson studies, again at satura-

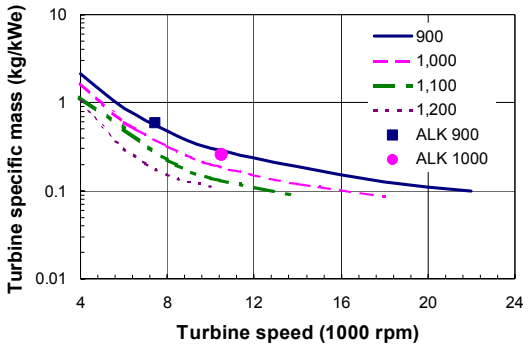

Figure B-1. Comparison of specific mass values for potassium Rankine cycle turbines operating at 1,350 K inlet temperature and the outlet temperatures (K) shown. Line data were calculated by Hudson while the symbol data were found by ALKASYSM.

tion pressure, and were 900 and 1,000 K for the two ALKASYS cases matching the criteria described. Blade tip speed in the ALKASYSM data was set at 1,000 ft/s.

For the 900-K data, the agreement between the Hudson model and the ALKASYSM model is excellent. It appears that with a blade tip speed limit of 1,000 ft/s, ALKASYSM overestimates by about a third with respect to the Hudson model at the higher turbine outlet temperature. However, from the coarseness of each model, neither has an inherent claim to the greater accuracy. Because the 900-K case is not far from the 800-K baseline for comparison between Rankine and Brayton systems, the agreement between these two models adds a measure of confidence in the result for that temperature.

The size of the turbine and generator computed by the ALKASYSM code is dependent on the tip velocity assumed. The models will give different results for most conditions because the criteria for setting that parameter are different. In the ALKASYSM code, the value may be entered as a fixed constant, or it may appear as a local Mach number. In the Hudson model, it is adjusted based on allowed stresses. To examine the influence of blade tip speed in the ALKASYS case, the code was adjusted slightly to allow the tip velocity to be input as a fraction of local sonic velocity or Mach number. Figure B-2 shows the results of varying the Mach number at the blade tip for a turbine/generator set assumed to be one fourth of a system that produced 15 MW_e from potassium boiling at 1,350 K. The reference case data are for 1,000 ft/s as used in Figure B-1.

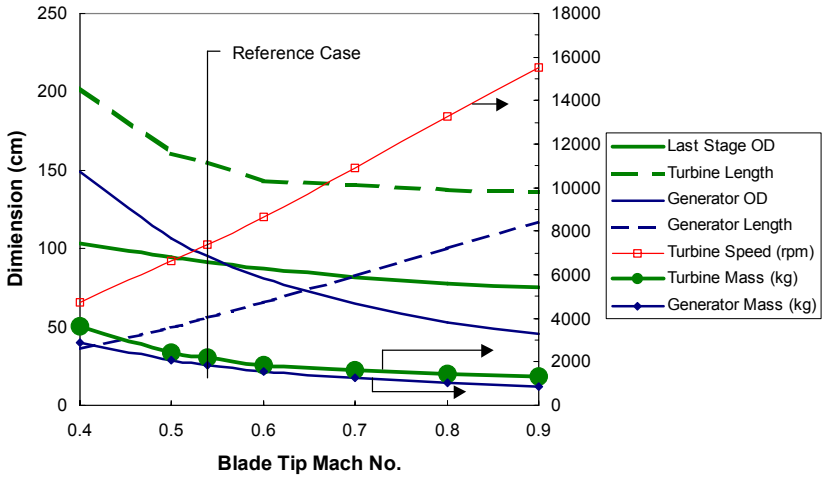

Figure B-2. Dimensions (left axis), masses, and rotational speeds (right axis) calculated by ALKASYSM over a range of last-stage blade tip Mach numbers for a turbine and generator comprising one fourth of the 15 MW_e Rankine power system taken as the baseline for comparison.

It is not surprising that diameters of both the turbine and the alternator/generator decrease with increasing rotational speed. Turbine length also decreases, but generator length increases with increasing rotational speed. It is also not surprising that turbine mass and generator mass are nearly equal.

As a check, the blade root stresses and disk stresses were calculated for these cases using Equations (B-11) and (B-12) above from Hudson's model. Results are shown in Figure B-3.

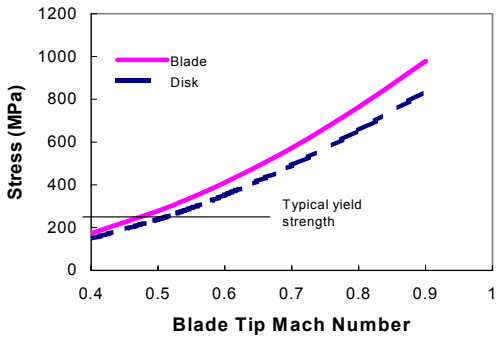

Figure B-3. Stresses in ALKASYS turbine estimated using Hudson's equations.

It is evident that, for these conditions, allowing higher blade-tip speeds than the 1,000 ft/s (Mach 0.539) used in the reference case will exceed allowable stress limits for typical yields strengths for high-temperature alloys. Further-more, it seems prudent to ensure that the flow from the nozzle is subsonic. Therefore, under the assumptions that the spouting velocity is twice that of the blade at its mean radius and that the tip radius is twice the hub radius, the tip Mach number should probably remain below 0.6.

A further interesting note from Hudson, based on comparative calculations performed and reported by him, is that "Rankine turbines are 3 to 4 times more massive than the corresponding Brayton turbines, providing the turbines are constrained to operate at the same speed and are made of the same … materials"[B4]

A conclusion from these comparisons is that the turbine/generator masses estimated by the ALKASYSM code are realistic though probably conservative.

APPENDIX B REFERENCES

B1. General Electric Power Systems Internet site http://gepower.com/products/prod_specs.htr., February 8, 2001.

B2. R. E. Morgan et al., ""Comparison of High Power Nuclear Systems for Space Application," *Proceedings of the 18th Intersociety Energy Conversion Engineering Conference,* Orlando, Florida, August 21-26, 1983, pp. 977-982.

B3. J. C. Moyers and J. P. Nichols, *ALKASYS, A Computer Program for Studies of Rankine Cycle Space Nuclear Power Systems,* ORNL/TM-10427, September 1987, Oak Ridge National Laboratory, Oak Ridge, TN.

B4. S. L. Hudson, "A Simplified Sizing and Mass Model for Axial Flow Turbines," *Proceedings of the 24th Intersociety Energy Conversion Engineering Conference,*IECEC-89, August 6–11, 1989, Washington, D.C., Institute of Electrical and Electronics Engineers., pp. 1091–1096.